Daniel-Sebastian Dohle, Thomas Zumbrink, Michael Meißner and Herbert P. Jennissen*

Protein Adsorption Hysteresis and Transient States of Fibrinogen and BMP-2 as Model Mechanisms for Proteome-Binding to Implants

Abstract: Protein adsorption studies returned to the focus of medical therapeutics, when it was found that up to 2500 *non-plasma proteins* adsorbed to hip implants during arthroplastic surgery, challenging peri-implant healing models. Questions have re-emerged as to the implications of uncontrolled protein unfolding after adsorption. In past studies on the cooperativity of protein binding we discovered protein adsorption hysteresis, a thermodynamically irreversible process. The present precursory study comprises real-time kinetic (TIRF-Rheometry) and equilibrium (^{125}I-tracer) studies on the hysteretic binding of fibrinogen and rhBMP-2 to titanium and glass surfaces via transient states. Thermodynamic constants ($\Delta G^{O''}$), as well as kinetically derived (K'_A) and hysteresis derived (K'_{HA}) association constants in the range of 10^6 to 10^{12} M^{-1} lead to a consistent picture.

Keywords: adsorption and desorption isotherms, total internal reflection fluorescence (TIRF), TIRF-rheometry, binding constants, Hill constants, on-rate (k_{+1}), off-rate (k_{-1})

https://doi.org/10.1515/cdbme-2020-3046

1 Introduction

Recently we published the proteomic composition (implantome) of the first protein layer on hip implant shafts intra-surgically retrieved after 2 min for the first time [1,2]. The implantome consisted of 2802 protein entities. The adsorption of proteins on surfaces generally occurs in the form of an adsorption-desorption hysteresis loop [3,4]. The desorption isotherm does not retrace the adsorption isotherm as a result of thermodynamic irreversibility. In the two-state domain model of a hysteresis cycle the apparent binding constants (K'_A) for the adsorption and desorption branches of the hysteresis loop can be calculated. The evaluation of hysteretic data is based on the model-assumption that the long-lived metastable states of the local energy minima can be treated thermodynamically as true equilibria ([5]).

***Corresponding author:**

Prof. Dr. H. P. Jennissen, Institut für Physiologische Chemie, und am Lehrstuhl Orthopädie und Unfallchirurgie, Universität Duisburg-Essen, Universitätsklinikum Essen, Hufelandstr. 55, D-45122 Essen, Germany; Email: hp.jennissen@uni-due.de

Daniel-S. Dohle[1,2], Thomas Zmbrink[1] and Michael Meißner[1]

[1]Institut für Physiologische Chemie, AG Biochemische Endokrinologie

[2]Klinik und Poliklinik für HTG-Chirurgie, Universität Mainz, D-55131 Mainz, Germany

2 Materials and Methods

Proteins. Bovine fibrinogen (*m* = 340 kDa [6]; 95-98% clottability) was purified from frozen bovine blood plasma by classical means as described in [6] and stored at -80°C. Human fibrinogen (95-98% clottability) was purified from human blood plasma by critical hydrophobicity hydrophobic interaction chromatography (HIC) in one step [6]. Recombinant human bone morphogenetic protein (rhBMP-2; *m* = 26 kDa [10]) was prepared in *E. coli* [7,8] with a *biological activity equivalent* ($K'_{0.5}$) of 2-10 nM [9,10].

Batch Measurements on titanium miniplates. Electrolytically polished titanium miniplates (5 x 10 x 1 mm) were cleaned with acetone as described (advancing contact angle 70-80°) [11]. Human fibrinogen was radioactively labelled by ^{125}I according to McFarlane [12] and stored at -80°C. As shown by Schmitt et al. [13] ^{125}I fibrinogen labelled by the iodine monochloride method shows no preferential adsorption in comparison to the non-labelled species.

Adsorption isotherms (Langmuir and Freundlich types) [3] were determined in **buffer A** (50 mM Tris, 150 mM NaCl, 1 mM EDTA, pH 7.4) by incubation of acetone treated miniplates in solutions of increasing ^{125}I-fibrinogen concentrations until apparent adsorption equilibrium after 12 hours and measuring the bound radioactive fibrinogen.

For desorption isotherms ^{125}I-fibrinogen loaded miniplates were incubated in defined volumes (2-200 ml) of sterile **buffer A** solutions for 48 hours to apparent desorption equilibrium at decreasing concentrations followed by analysis of residually bound ^{125}I-fibrinogen. The Freundlich isotherms were converted to the Hill isotherms [3] and the half-saturation constant K_{HD} (= $K_{0.5}$) was calculated from the Hill constant according to $K_H = (K_{0.5})^{n_H}$ [3]. The reciprocal of K_{HD} [M] is the here employed association constant K_{HA} [M^{-1}]. In the desorption kinetic studies readsorption was prevented by a continous flow-through system.

TIRF-Rheometer [14] analysis on quartz glass. Highly polished quartz glass discs (Suprasil I, Ra ~1-3 nm, ∅ = 36 mm, 0.9 mm thick) were cleaned in chromosulfuric acid (CSA) as described (θ_{Adv} = 0-10°) [15]. Kinetic measurements of bovine fibrinogen (95-98% clottability) were performed in **buffer A** by total internal reflection fluorescence (TIRF) utilizing the air-bubble technique (BLEB [16]) in a flow-through TIRF-Rheometer cell [15,16], employing a Spex Fluorolog spectrometer Model F112 (Instruments SA, München) with a xenon lamp (excitation: λ = 290 nm, emission: λ = 350 nm) for analysis of tryptophan fluorescence [15]. Solutions of rhBMP-2 (e.g. 0.1 mg/ml, 3.8µM) were adsorbed and desorbed in 50 M sodium acetate buffer, pH = 4.5 (**buffer B**). After obtaining adsorption equilibrium in ca. 5 min rhBMP-2 was desorbed for 20 h.

The resulting exponential adsorption kinetics at increasing concentrations yield a series of observed rate constants (k_{obs}) from which the on-rate (k_{+1}) and off-rate (k_{-1}) constants can be calculated. Since the observed transient protein states are metastable [3,4] the derived constants are labeled as "apparent" by (') [3] e.g. K' as K-prime.

Thermodynamic evaluation. Long-lived metastable states, corresponding to local energy minima, can be treated thermodynamically as true equilibria (see [3,5]), allowing the calculation of apparent standard Gibbs free energies (double prime): $\Delta G^{O''} = -RT \ln K'$ (R = 8.314472 J/K^{-1} mol^{-1}; absolute Temperature T = 298 K (= RT 25 °C); the ln of the constants K'_A, K'_{HA}. For curve fitting and statistical analysis the PC program Graphpad Prism Vers. 4. was employed.

3 Results and Discussion

3.1 Adsorption Hysteresis of ^{125}I-Fibrinogen on Titanium Miniplates

Although adsorption isotherms of fibrinogen on titanium and glass can often be fitted to hyperbolas [17], they are not true Langmuir isotherms, since the fundamental postulates of Langmuir are not fulfilled [18,19]. In **Fig. 1A** one adsorption isotherm (solid symbols) and three desorption isotherms (open symbols, so-called *scanning curves*) of fibrinogen hysteresis on miniplates are shown in a double log plot as Freundlich isotherms (no chemisorption as in [17]). The desorption isotherms originate at the *upper closure point* (special symbols). For the adsorption isotherm a K'^{A}_{HA} = 2.6 x 10^6 M^{-1} and for the top desorption isotherm a K'^{D}_{HA} = 2.9 x 10^{11} M^{-1} are obtained. In **Fig. 1B** two first order off-rate constants of a two-phase exponential desorption (k_{-1} = 1.2 x 10^{-5} s^{-1} and k_{-2} = 2.6 x 10^{-7} s^{-1}) are derived. It is assumed, that the uncertainty in calculating the apparent binding constants (K'_A) from the on-rate constant on polished glass (**Fig. 2**) and the off-rate constants on polished titanium (**Fig. 1B**) is tolerable. The constants derived from **Fig. 1** are shown in **Table 1** indicating four transient states. From the difference of the two app. standard Gibbs free energies of adsorption ($\Delta G_a^{O''}$ = -36.0 kJ mol^{-1}) and desorption ($\Delta G_d^{O''}$ = -64.3 kJ mol^{-1}) an

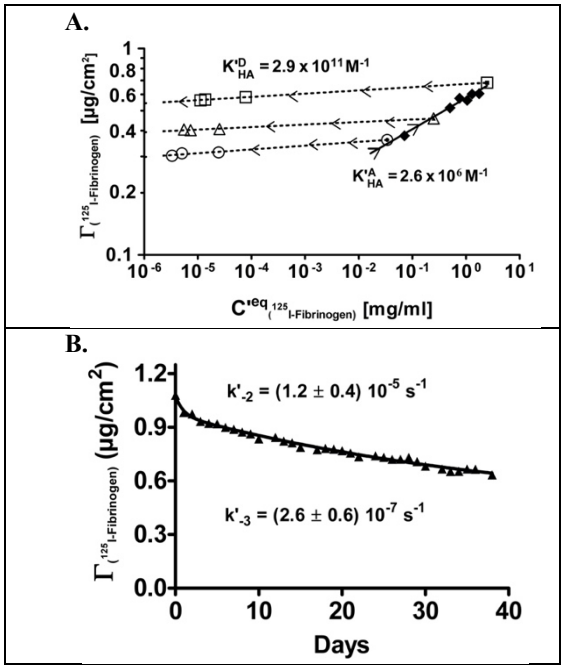

Fig. 1
Protein adsorption-desorption hysteresis of ^{125}I-fibrinogen at apparent equilibria and release kinetics on titanium miniplates.
***A**. Adsorption isotherm (◆) and (⊙, ▣, △), arrows upward Desorption isotherms (○, □, △), arrows downward upper closure points (⊙, ▣, △); Γ: surface concentration*
***B**. Desorption kinetics of ^{125}I-fibrinogen from titanium miniplates fitted to a two-phase exponential equation. For further details and constants see **Table 1,** Methods and ref. [3].*

irreversible change of $\Delta iG^{O''}$ = -28.3 kJ mol^{-1} can be calculated, the energy cost of multivalence-caused conformational change. For the difference of the transient states 03 and 04

Table 1
*Equilibrium and kinetic constants derived from **Fig. 1**.*

^{125}I-Fibrinogen (Adsorption-Desorption Hysteresis)				
Sorption States	k'_{+1} M^{-1} s^{-1}	k'_{off} s^{-1}	K'_{HA} K'_A M^{-1}	$\Delta G^{O''}$ kJmol^{-1}
State 01 (**Fig. 1A**)	-	-	2.6 x 10^6	-36.0
State 02 (**Fig. 1A**)	-	-	2.9 x 10^{11}	-64.3
State 03 (**Fig. 1B**)	*3.4 ± 0.5* x 10^5*	1.2 ± 0.4 x 10^{-5}	2.8 x 10^{10}	-58.6
State 04 (**Fig. 1B**)	*3.4 ± 0.5* x 10^5*	2.6 ± 0.6 x 10^{-7}	1.3 x 10^{12}	-68.0

On-rate constants of **Fig. 2A.; mean ± S.D.*

(**Table 1**) an apparent dissipated Gibbs free energy of $\Delta iG^{O''}$ = -9.4 kJ mol^{-1} is obtained. The $\Delta G_d^{O''}$ = -58.6 kJ mol^{-1} (298 K) of state 03 is in good agreement with the voltammogramic values of ΔG^O_{ADS} = -54.2 kJ mol^{-1} (310 K) in [17]. In comparison the hydrolysis of ATP yields $\Delta G^{O'}$ ~ -30 kJ mol^{-1}.

3.2 Evanescent Wave Kinetics of Fibrinogen on Quartz Glass

In **Fig. 2A** the k_{obs}-values derived from separate exponential adsorption kinetics of fibrinogen on quartz glass via TIRF-rheometry (see [15]) are plotted as a linear function versus the initial fibrinogen concentration. The apparent on-rate constant k'_{+1} = 3.4 x 10^5 M^{-1}s^{-1} [15] is obtained from increment and the off-rate constant (k'_{-1} = 8.1 x 10^{-2}) from the intersect with the ordinate. The on-rate constant (k'_{+1}) also allows an unbiased calculation of the binding constants from the off-rate constants of **Fig. 2B** (see **Table 2**). It appears that the final affinity of fibrinogen for the titanium surface (**Table 1**) is ca. one order of magnitude higher than for glass. The affinity of fibrinogen in state 01 with a binding constant of 4.1×10^6 M^{-1} increases versus state 02 by over two-orders of magnitude with a $\Delta iG^{O''}$ = -14.7 kJ mol^{-1} and versus state

Table 2

*Equilibrium and kinetic constants for three fibrinogen transient states on quartz glass as measured by evanescent wave technology [15] derived from **Fig. 2**.**

Fibrinogen (TIRF-Rheometry)				
Sorption States	k'_{+1} M^{-1} s^{-1}	k'_{-1} s^{-1}	K'_A M^{-1}	$\Delta G^{O''}$ kJmol^{-1}
State 01 (**Fig. 2A**)	3.4 ± 0.5 x 10^5	8.1 ± 0.02 x 10^{-2}	4.1 x 10^6	-37.1
State 02 (**Fig. 1B**)	3.4 ± 0.5 x 10^5	2.0 ± 0.6 x 10^{-4}	1.7 x 10^9	-51.8
State 03 (**Fig. 2B**)	3.4 ± 0.5 x 10^5	5.9 ± 3.0 x 10^{-6}	5.7 x 10^{10}	-60.4

mean ± S.D.

3.3 Evanescent Wave Kinetics of rhBMP-2 on Quartz Glass

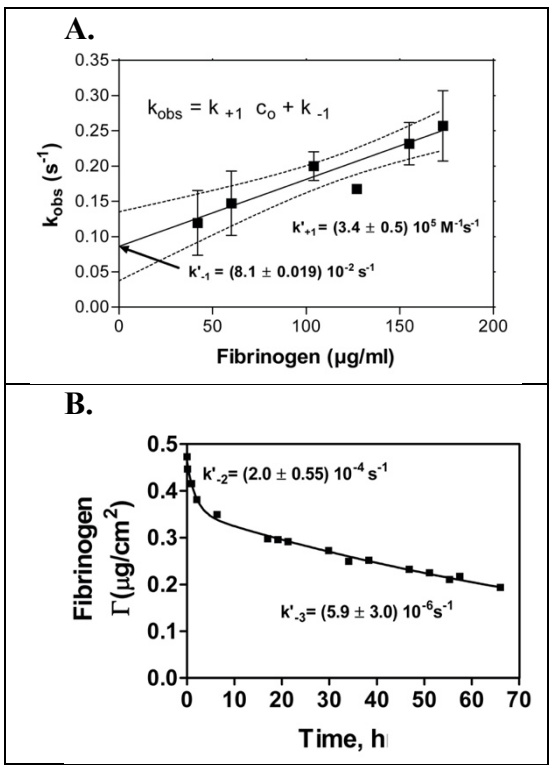

Fig. 2

Determination of apparent adsorption and desorption rate constants of fibrinogen on quartz glass by TIRF-Rheometry.

***A**. k_{obs}-plot for the determination of k'_{+1} and k'_{-1} of the initial complex. Dashed lines: boundaries for 95% confidence.*

***B.** The two-phase exponential desorption from the quartz glass was measured by TIRF under conditions of minimal bleaching and correction of quenching (**A.** from ref. [15]).*

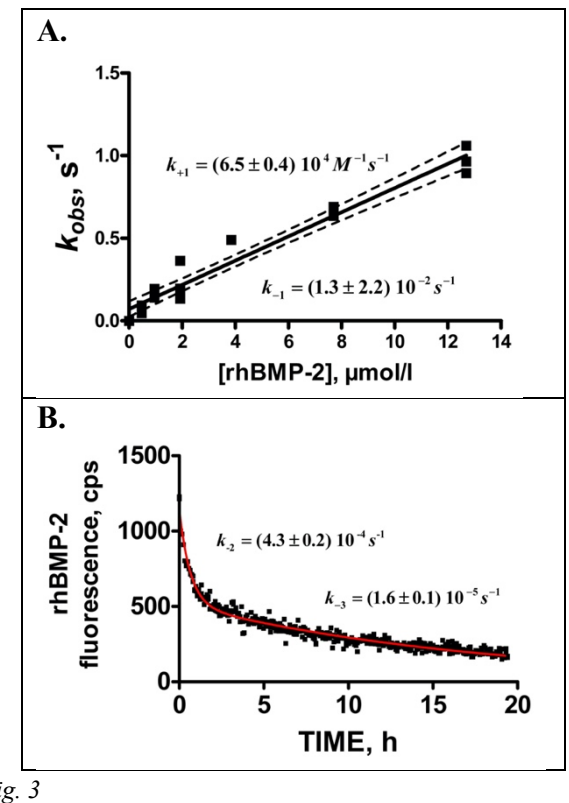

Fig. 3

Determination of apparent adsorption and desorption rate constants of rhBMP-2 on quartz glass by TIRF-Rheometry.

***A.** k_{obs}-plot for the determination of k'_{+1} and k'_{-1} of the initial complex. Dashed lines: boundaries for 95% confidence.*

***B.** Two-phase exponential desorption of rhBMP-2 in quartz glass TIRF-cell after 5 min in residence following saturating exponential adsorption (~50 s) under conditions of minimal bleaching and correction of quenching (see ref. [15]).*

03 by another order of magnitude $\Delta iG^{O''} = -8.6$ kJMol^{-1}. Thus three transient states of fibrinogen cover ca. four orders of magnitude at a cost of ca. $\Delta iG^{O''} = -23.3$ kJ mol^{-1}. The values of $\Delta G^{O''}$ =-52 to -60 kJ mol^{-1} (**Table 2**) are in good agreement with the voltammogramic ΔG^{O}_{ADS} = -52 to -55 kJ mol^{-1} [17].

A kinetic analysis of the adsorption of rhBMP-2 on quartz glass is shown in **Fig. 3**. This is of interest since rhBMP-2 has been adsorbed on titanium surfaces for the preparation of successful bioactive implants in sheep [7]. The cystine-knotted BMP-2 molecule might resist adsorption hysteresis and possibly unfolding on surfaces. As derived from **Fig. 3** and **Table 3**, the rhBMP-2 molecule runs through similar transient states 01 and 02 ($\Delta iG^{O''} = -8.3$ kJ mol^{-1}) followed by states 02 and 03 ($\Delta iG^{O''} = -5.4$ kJMol^{-1}) with affinities over three orders of magnitude similar to fibrinogen. A $\Delta G^{O''} = -51.3$ kJ mol^{-1} compares to ca. 13 H-bonds. Referable adsorption rate constants for proteins of $k_{on} \sim 10^5$ M^{-1} s^{-1} were published by Aptel et al. [20]. Desorption rate constants in the range of 10^{-4} - 10^{-6} s^{-1} have been reported by Huetz et al. [21].

Table 3

*Equilibrium and kinetic constants derived from **Fig. 3***.*

rhBMP-2 (TIRF-Rheometry)				
Sorption States	k'_{+1} M^{-1} s^{-1}	k'_{-1} s^{-1}	K'_A M^{-1}	$\Delta G^{O''}$ kJ mol^{-1}
State 01 (Fig. 3A)	6.5 ± 0.4 x 10^4	1.3 ± 2.2 x 10^{-2}	5.0 x 10^6	-37.6
State 02 (Fig. 3B)	6.5 ± 0.4 x 10^4	4.3 ± 0.2 x 10^{-4}	1.5 x 10^8	-45.9
State 03 (Fig. 3B)	6.5 ± 0.4 x 10^4	1.6 ± 0.1 x 10^{-5}	1.4 x 10^9	-51.3

**mean ± S.D.*

Acknowledgements

The support of the Deutsche Forschungsgemeinschaft (DFG Reference No. Je84/15-3) is gratefully acknowledged.

Author Statement

The Authors state no conflict of interest.

4 References

[1] Jäger, M., Jennissen, H. P., Haversath, M., Busch, A., Grupp, T., Sowislok, A., & Herten, M. (2019) Intra-surgical Protein Layer on Titanium Arthroplasty Explants: From the Big Twelve To The Implant Proteome. *Proteomics. Clin. Appl.*, e1800168 (pp. 1-16); (DOI: 10.1002/prca.201800168).

[2] Jennissen, H. P. (2019) Implantomics: A Paradigm Shift in Implantology. *Curr. Dir. Biomed. Engineer.*, **5,** 131-136.

[3] Jennissen, H. P. & Botzet, G. (1979) Protein binding to two-dimensional hydrophobic binding-site lattices: Adsorption hysteresis on immobilized butyl-residues. *Int J Biol Macromol*, **1,** 171-179.

[4] Jennissen,H.P. (1985) Protein Adsorption Hysteresis. In *"Surface and Interfacial Aspects of Biomedical Polymers" Vol.2, Protein Adsorption* (Andrade,J.D., ed), pp. 295-320. Plenum Press, New York.

[5] Katchalsky, A. & Spangler, R. (1968) Dynamics of membrane processes. *Quart. Rev. Biophys.*, **1,** 127-175.

[6] Jennissen, H. P. & Demiroglou, A. (2006) Interaction of fibrinogen with n-alkylagaroses and its purification by critical hydrophobicity hydrophobic interaction chromatograpy. *J Chromatogr. A*, **1109,** 197-213.

[7] Chatzinikolaidou, M., Lichtinger, T. K., Müller, R. T., & Jennissen, H. P. (2010) Peri-implant reactivity and osteoinductive potential of immobilized rhBMP-2 on titanium carriers. *Acta Biomater.*, **6,** 4405-4421.

[8] Jennissen, H. P., Zumbrink, T., Chatzinikolaidou, M., & Steppuhn, J. (1999) Biocoating of Implants with Mediator Molecules: Surface Enhancement of Metals by Treatment with Chromosulfuric Acid. *Materialwiss. Werkstofftech. (Mater. Sci. Eng. Technol.)*, **30,** 838-845.

[9] Wiemann, M., Rumpf, H. M., Bingmann, D., & Jennissen, H. P. (2001) The Binding of rhBMP-2 to the Receptors of viable MC3T3 Cells and the Question of Cooperativity. *Materialwiss. Werkstofftech. (Mat. Sci. Engineer. Technol.)*, **32,** 931-936.

[10] Laub, M., Chatzinikolaidou, M., & Jennissen, H. P. (2007) Aspects of BMP-2 Binding to Receptors and Collagen: Influence of Cell Senescence on Receptor Binding and Absence of High-Affinity Stoichiometric Binding to Collagen. *Materialwiss. Werkstofftech. (Mat. Sci. Engineer. Technol.)*, **38,** 1020-1026.

[11] Chatzinikolaidou, M., Laub, M., Rumpf, H. M., & Jennissen, H. P. (2002) Biocoating of Electropolished and Ultra-Hydrophilic Titanium and Cobalt Chromium Molybdenium Alloy Surfaces with Proteins. *Materialwiss. Werkstofftech. (Mater. Sci. Eng. Technol.)*, **33,** 720-727.

[12] McFarlane, A. S. (1963) In Vivo Behavior of I-Fibrinogen. *J Clin. Invest*, **42,** 346-361.

[13] Schmitt, A., Varoqui, R., Uniyal, S., Brash, J. L., & Pusineri, C. (1983) Interaction of fibrinogen with solid surfaces of varying charge and hydrophobic-hydrophilic balance. *Journal of Colloid and Interface Science*, **92,** 25-34.

[14] Jennissen, H. P., Sanders, A., Schnittler, H. J., & Hlady, V. (1999) TIRF-Rheometer for Measuring Protein Adsorption Under High Shear Rates:Constructional and Fluid Dynamic Aspects. *Materialwiss. Werkstofftech. (Mater. Sci. Eng. Technol)*, **30,** 850-861.

[15] Jennissen, H. P. & Zumbrink, T. (2004) A Novel Nanolayer Biosensor Principle. *Biosens. Bioelectron.*, **19,** 987-997.

[16] Jennissen, H. P. (2005) Boundary-Layer Exchange by Bubble: A Novel Method for Generating Transient Nanofluidic Layers. *Physics of Fluids*, **17,** 100616-1-100616-9.

[17] Jackson, D. R., Omanovic, S., & Roscoe, S. G. (2000) Electrochemical Studies of the Adsorption Behavior of Serum Proteins on Titanium. *Langmuir*, **16,** 5449-5457.

[18] Langmuir, I. (1940) Monolayers on solids. *J Chem Soc London*, **1940,** 511-543.

[19] Jennissen, H. P. (1981) Immobilization of residues on agarose gels: Effects on protein adsorption isotherms and chromatographic parameters. *J Chromatogr*, **215,** 73-85.

[20] Aptel,J.D., Carroy,A., Dejardin,P., Pefferkorn,E., Schaaf,P., Schmitt,A., Varoqui,R., & Voegel,J.C. (1987) Adsorption and Desorption of Synthetic and Biological Macromolecules at Solid-Liquid Interfaces: Equilibrium and Kinetic Properties. In *Proteins at Interfaces: Physicochemical and biochemical Studies, ACS Symposium Series 343* (Brash,J.L. & Horbett,T.A., eds), pp. 222-238.

[21] Huetz, P. H., Ball, V., Voegel, J. C., & Schaaf, P. (1995) Exchange Kinetics for a Heterogeneous Protein System on a Solid Surface. *Langmuir*, **11,** 3145-31.